

## Determination of Correlation Times of New Paramagnetic Gadolinium MR Contrast Agents by EPR and $^{17}\text{O}$ NMR

Hee-Kyung Kim,<sup>†</sup> Gang-Ho Lee,<sup>‡</sup> Tae-Jeong Kim,<sup>§,\*</sup> and Yongmin Chang<sup>†,\*</sup>

<sup>†</sup>Department of Medical & Biological Engineering, Kyungpook National University, Daegu 702-701, Korea

<sup>‡</sup>Department of Chemistry, Kyungpook National University, Daegu 702-701, Korea

<sup>§</sup>Department of Applied Chemistry, Kyungpook National University, Daegu 702-701, Korea. \*E-mail: tjkim@knu.ac.kr

<sup>†</sup>Department of Molecular Medicine, Kyungpook National University, Daegu 702-701, Korea

Received January 15, 2009, Accepted February 19, 2009

The work describes EPR and  $^{17}\text{O}$  NMR measurements followed by theoretical calculation of the rotational correlation time ( $\tau_R$ ), the water residence time ( $\tau_m$ ), and the longitudinal electronic spin relaxation time ( $T_{1e}$ ) for two new gadolinium complexes **1** and **2** of the type  $[\text{Gd}(\text{L})(\text{H}_2\text{O})]$  (L = tranexamic esters) in order to investigate their efficiency as a paramagnetic contrast agent (PCA). Of three correlation times,  $\tau_R$  plays a major and predominant role to the unusually high relaxivity of **1** and **2** as compared with that of clinically approved MR CAs such as  $[\text{Gd}(\text{DTPA})(\text{H}_2\text{O})]^{2-}$  (Magnevist<sup>®</sup>),  $[\text{Gd}(\text{DTPA-BMA})(\text{H}_2\text{O})]$  (Omniscan<sup>®</sup>), and  $[\text{Gd}(\text{DOTA})(\text{H}_2\text{O})]$  (Dotarem<sup>®</sup>). The presence of bulky tranexamic ester in the ligand seems to be responsible for the conformational rigidity, which in turn causes such great an increase in  $\tau_R$ .

**Key Words:** MRI CA, Gadolinium chelate, Tranexamate, Correlation times

### Introduction

Magnetic resonance imaging (MRI) provides high resolution, three-dimensional images of the internal part of the body depending on the difference in the *in vivo* distribution of the water molecules. The relatively low sensitivity of MRI can be overcome by inducing additional contrast in the MR images by the introduction of a paramagnetic contrast agent (PCA) prior to the MRI test.<sup>1</sup> These paramagnetic agents catalytically shorten the longitudinal relaxation time ( $T_1$ ) of the nearby water molecules to enhance the contrast with the background tissues in the MR images.  $T_1$  relaxivity defined as  $1/T_1$  per millimolar-second is therefore a measure representing the efficiency of PCA. Relaxivity of PCA is determined by three physicochemical factors: (i) the rotational correlation time ( $\tau_R$ ) of the complex, (ii) the water residence time ( $\tau_m$ ) in the inner sphere, and (iii) the longitudinal electronic spin relaxation time ( $T_{1e}$ ) of paramagnetic ion.<sup>2-11</sup>

It is worth mentioning that  $T_{1e}$ , although provides quite critical information in certain cases, is too short to be directly measured by current EPR techniques.<sup>12</sup> Nevertheless, the decay of the electronic spin magnetization perpendicular to the external field, usually characterized by a transverse electronic relaxation time ( $T_{2e}$ ), allows an estimation of  $T_{1e}$  within the framework of a given model of the electronic relaxation.<sup>13</sup> For this purpose, variable temperature EPR measurements were performed to obtain detailed information about the dynamics of the system. Some empirical formulas, initially proposed by Powell to describe both transverse and longitudinal relaxation times, have been applied in a unified model to simultaneously interpret  $^{17}\text{O}$  NMR,  $^1\text{H}$  NMR, and EPR.<sup>4,8,9</sup> Yet, Powell's formulas have exhibited some drawbacks in that they not only require an additional factor such as a spin rotation mechanism for the interpretation of data but also the final results thus obtained are generally in a poor

agreement with the experimental EPR data. Thus, for the purpose of reasonable prediction of  $T_{1e}$ , it is desirable to find a suitable model enabling to describe the underlying mechanism. In this regard, it is worth noting that Rast has recently developed a refined model of the electronic relaxation of the S states of metal ion complexes in solution.<sup>14-16</sup> This model includes the contribution of the static crystal field surrounding the Gd(III) ion caused by its modulation by the rotation of the whole complex besides a part due to the usual transient crystal zero-field splitting (ZFS) caused by vibration, intramolecular rearrangement, and collision with surrounding solvent molecules. A good agreement with the measured peak-to-peak width was observed for such complexes as  $[\text{Gd}(\text{H}_2\text{O})_9]^{3+}$ ,  $[\text{Gd}(\text{DTPA})(\text{H}_2\text{O})]^{2-}$ , and  $[\text{Gd}(\text{DTPA-BMA})(\text{H}_2\text{O})]$  over a wide range of temperatures.<sup>14</sup> It is the Rast's model that provides a realistic relaxation model including the effects of the static crystal field and of the transient zero field splitting.<sup>13-15</sup>

We have been involved for some time in the design and the synthesis of some new DTPA-bis(amides) and their gadolinium complexes for use in MRI.<sup>17-18</sup> In one case, we have observed that gadolinium complexes of DTPA-bis(amide) conjugates of tranexamic esters, **1** and **2** (Chart 1), exhibit much higher  $T_1$  relaxivity with the highest value reaching up to 2.6 times as high as that for Omniscan<sup>®</sup>.<sup>19</sup> Motivated by these observations, we have performed EPR and  $^{17}\text{O}$  NMR experiments to determine three correlation times ( $\tau_R$ ,  $\tau_m$ ,  $T_{1e}$ ) of **1**, **2**, and other clinically used MR CAs such as Magnevist<sup>®</sup>, Omniscan<sup>®</sup>, and Dotarem<sup>®</sup> for comparative purposes.

### Experimental Section

**Sample preparation.** The complexes **1** and **2** were prepared according to the literature method.<sup>17</sup>  $[\text{Gd}(\text{DTPA})(\text{H}_2\text{O})]^{2-}$  (Magnevist<sup>®</sup>, Schering),  $[\text{Gd}(\text{DTPA-BMA})(\text{H}_2\text{O})]$  (Omniscan<sup>®</sup>, Sanofi Nycomed), and  $[\text{Gd}(\text{DOTA})(\text{H}_2\text{O})]$  (Dotarem<sup>®</sup>, Guer-

bet) were purchased and used without further purification. In all  $^{17}\text{O}$  NMR measurements, 20%  $^{17}\text{O}$  enriched water (ISOTEC, INC) was added to the solutions to improve sensitivity.

**EPR experiment and computational program.** The EPR spectra were measured at X-band (JEOL, JES-TE300) and operated in a continuous wave mode. The samples were prepared in a flat cell. The peak-to-peak line width was measured from the recorded spectrum using the MATLAB program. The cavity temperature was stabilized by electronic temperature control of gas flowing through the cavity, and measurements made in the temperature range 278–333K. A program which performs a fit of the zero field splitting parameters was supplied by Alain Borel, Ecole Polytechnique Federale de Lausanne, Switzerland.<sup>12,13</sup> The program was compiled in the Matlab 6.5 of Linux redhat enterprise edition 5.

**EPR theoretical model section.** The Rast's model employed in this study can be derived from Redfield's relaxation theory. The Hamiltonian of the system is written in the laboratory frame (eq 1).

$$\hbar H(t) = \hbar H_0 + \hbar H_1^{(L)}(t) \quad (1)$$

$\hbar H_0 = \hbar \omega_0 S_z$  is a time-dependent Zeeman effect term, and  $\omega_0$  a Larmor frequency.<sup>15</sup> Second term is written from the sum of a static zero field splitting (ZFS) and a transient ZFS (eq 2).

$$H_1^{(L)}(t) = H_{1S}^{(L)}(t) + H_{1T}^{(L)}(t) \quad (2)$$

In the molecular frame, the best known form of the operators  $H_{1S}^{(M)}$  and  $H_{1T}^{(M)}(t)$  is the second order expression as in eq (3)

$$\begin{aligned} H_1 &= D \left[ S_z^2 - \frac{1}{3} S(S+1) \right] + E \left[ S_x^2 - S_y^2 \right] \\ &= \sqrt{\frac{2}{3}} D T_2^0 + E \left[ T_2^{-2} + T_2^2 \right] \end{aligned} \quad (3)$$

with real coefficients D, E. The magnitude of the ZFS is then characterized by the parameter  $\Delta$  defined as eq (4).<sup>20</sup>

$$\Delta^2 \equiv \frac{2}{3} D^2 + 2E^2 \quad (4)$$

The spectrum of EPR is that of energy absorbed by electrons and can be expressed as a correlation function,  $G_x(t)$  which is an even and real function. Thus, its Fourier transformed function,  $(\hat{G}_x(\omega))$  has the same property. Then, spectral density function is given as eq (5).<sup>14</sup>

$$F_x(\omega) = \text{Re}(\hat{G}_x(\omega)) = \text{Re} \int_{-\infty}^{\infty} G_x(t) e^{i\omega t} dt$$

The line width is defined as the peak-to-peak distance of the first derivative of the function  $F_x(\omega)$ . The eq (2) can also be expressed as a spectral density equation using the Wigner-Eckart theorem and 3j-symbols for each part of ZFS.<sup>14</sup> Consequently, the spectral density can be expressed in terms of a reduced number of independent adjustable parameters (eq 6).

$$a_k = \sqrt{\sum_{\alpha} (B_{k\alpha})^2} \quad k = 2, 4, 6 \quad \text{and} \quad a_{2T} = \sqrt{\sum_{\alpha} B_{2\alpha}^2(0)} \quad (6)$$

$B_{k\alpha}$  describes the magnitude of each contribution,  $\alpha$  is necessary supplementary index. The parameter  $a_2$  is an amplitude of the static zero-field splitting (ZFS) and  $a_{2T}$  an amplitude of the transient ZFS. It is not very useful to compare crystal field parameters  $a_2$  and  $a_{2T}$  to the ZFS parameter  $\Delta^2$  of previous works because  $\Delta^2$  reflects an averaged effect of the transient and static ZFS.<sup>8,9,11</sup>

The peak-to-peak EPR line-width ( $\Delta H_{PP}$ ) and other related independent parameters were fitted into the model. The independent parameters were adjusted by a mean square fit of  $\Delta H_{PP}$  with the experimental values,  $\Delta H_{PP}^{\text{exp}}$ . The value of  $F$  at the found minimum is denoted by  $F_{\text{min}}$ , (eq 7), and applied in order to give equal weights to all N experimental points at various fields and temperatures.<sup>14</sup>

$$F = \frac{1}{N} \sum_{i=1}^N \left[ \frac{\Delta H_{PP}(i) - \Delta H_{PP}^{\text{exp}}(i)}{\Delta H_{PP}^{\text{exp}}(i)} \right]^2 \quad (7)$$

The  $\tau_R$  and  $\tau_v$  values in eq (8) are defined according to the hypothesis of Merbach. The equation has an Arrhenius temperature dependence, where  $T_0 = 298.15\text{K}$  and  $E_R^{\ddagger}$ ,  $E_v^{\ddagger}$  are the activation energies for the rotational motion of the complex and for the transient ZFS, respectively. The activation energy for the rotation of the complex is about the same as for the hydrated  $\text{Gd}^{3+}$  complex. This is expected in the framework of the Stokes-Einstein model for a Brownian rotation in a viscous medium.  $\tau_R$  is the rotational correlation time related to static ZFS and  $\tau_v$  is vibrational correlation time related to transient ZFS. A slow rotational correlation time has been known to make relaxivity of Gd complex become higher.<sup>14</sup>

$$\tau_R(T) = \tau_R(T_0) e^{(E_R^{\ddagger}/Rk)(T-T_0)} \quad \text{and} \quad \tau_v(T) = \tau_v(T_0) e^{(E_v^{\ddagger}/Rk)(T-T_0)} \quad (8)$$

For the fitting, peak-to-peak width (G), central field (G), frequency (Hz), and concentration (M) for variable temperatures were used as input data. Supplied fitting program is based on the theory of Rast.<sup>14,16</sup> Concentration is set to 0 so that the concentration effect at X-band becomes negligible.<sup>14</sup> We fixed  $a_4 = a_6 = 0$  to reduce compensation effects between the parameters.<sup>14</sup>

**$^{17}\text{O}$  NMR experiment.** Variable temperature  $^{17}\text{O}$  NMR measurements were performed at 500 MHz using Varian Unity INOVA (11.8T, 67.814 MHz). The samples were sealed in glass spheres, fitting into 10 nm NMR tubes in order to eliminate susceptibility correction to the chemical shift. Transverse relaxation rates,  $1/T_2^*$  was obtained by the Carr-Purcell-Melboom-Gill (CPMG) technique. Variable temperature  $^{17}\text{O}$  NMR measurements were performed in the same temperature range as the case of EPR experiments.

## Results and Discussion

Table 1 shows ZFS parameters and  $T_1$ , fitted with parameters measured with **1** and **2** by EPR, along with the literature values of Magnevist<sup>®</sup>, Omniscan<sup>®</sup>, and Dotarem<sup>®</sup> for com-

**Table 1.** ZFS parameters and  $T_{1e}$  fitted with parameters measured from EPR spectrum at 298.15K<sup>a</sup>

	Magnevist <sup>®</sup>	Omniscan <sup>®</sup>	Dotarem <sup>®</sup>	1	2
$a_z (\times 10^{10} \text{ s}^{-1})$	0.87(0.92)	0.71(0.82)	0.40(0.35)	0.60	0.53
$a_{\text{ST}} (\times 10^{10} \text{ s}^{-1})$	0.54(0.43)	0.97(0.44)	0.67(0.43)	0.73	0.70
$\tau_R (\times 10^3 \text{ ps})$	3.02(3.95)	4.78(4.30)	4.01(4.91)	23.82	25.93
$\tau_v (\text{ps})$	1.51(1.33)	1.54(1.07)	0.57(0.54)	5.04	10.04
$E_R^A (\text{kJ}\cdot\text{mol}^{-1})$	18.20(12.6)	14.32(15.5)	19.0(16.4)	24.98	12.77
$E_v^A (\text{kJ}\cdot\text{mol}^{-1})$	16.13(15.7)	5.51(8.3)	9.58(6.0)	3.93	14.68
$F_{mn}$	0.0030(0.004)	0.0032(0.005)	0.0023(0.017)	0.0011	0.0014
$T_{1e} (\text{ns})$	0.36	0.39	1.37	0.38	0.36

<sup>a</sup>Data in the parentheses for Magnevist<sup>®</sup>, Omniscan<sup>®</sup>, and Dotarem<sup>®</sup> are taken from the literature.<sup>14,15</sup>

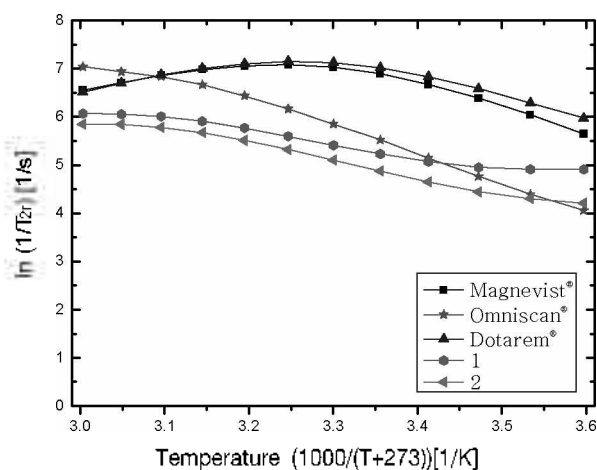
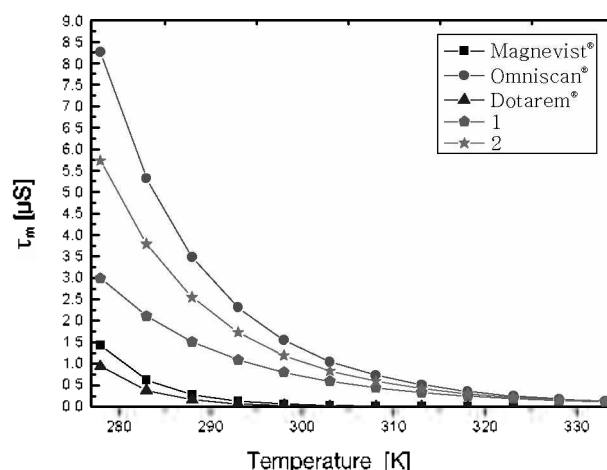
parative purposes. It has to be pointed out first of all that our fitting data for **1** and **2** are reliable as ZFS parameters are compared with those of three clinically approved MRI CAs.<sup>14,15</sup> Namely, all ZFS parameters for **1** and **2** fall within the range of those for the commercial CAs. Further confirmation for the reasonable fitting comes from the fact that the  $F_{mn}$  values for the new complexes are even lower than those for the reference values.

The most characteristic feature of the table is the unusually high rotational correlation time ( $\tau_R \times 10^3$  ps) for **1** and **2** reaching up to 23.82 and 25.93, respectively. At the same, it should also be noted that all but Dotarem<sup>®</sup> exhibit almost equal longitudinal electronic spin relaxation times ( $T_{1e}$ ) in the range of 0.36–0.39 ns; Dotarem<sup>®</sup> is exceptional to give 1.37 ns because it adopts a macrocyclic chelate rather than a linear one. These observations indicate that, of two parameters  $\tau_R$

and  $T_{1e}$ , the former plays a dominant role in the very high  $T_1$ -relaxivities of **1** and **2** as compared with the commercial MRI CAs. Exceptionally high  $\tau_R$  values for **1** and **2** may be explained in terms of the sterically demanding cyclohexyl moiety which retards the tumbling motion of the whole ligand.

In order to investigate the effect of the remaining parameter  $\tau_m$ , <sup>17</sup>O NMR experiments were performed. Related thermodynamic parameters such as the hyperfine coupling constant ( $A/\hbar$ ), the water-exchange entropy ( $\Delta S$ ), and the water-exchange enthalpy ( $\Delta H$ ) are obtainable by non-linear curve fitting of  $T_2$  relaxation data using MATLAB for use in the Swift-Connick<sup>21</sup> and Eyring equations.<sup>21,23</sup>

Figure 1 shows a plot of  $\ln(1/T_2)$  as a function of temperature, where  $T_2$  is the difference between transverse relaxation rates of the complex and bulk water. The figure shows that **1**, **2**, and Omniscan<sup>®</sup> exhibit a slow-exchange behavior in the

**Figure 1.** Temperature dependence of the <sup>17</sup>O transverse relaxation.**Figure 2.** Temperature dependence of water molecular residence time.**Table 2.** The parameters from non-linear curve fitting of  $T_2$  relaxation data

	Magnevist <sup>®</sup>	Omniscan <sup>®</sup>	Dotarem <sup>®</sup>	1	2
$A/\hbar (\times 10^7 \text{ rad}\cdot\text{s}^{-1})$	7.70	9.39	13.16	7.68	6.81
$\Delta S (\text{J}\cdot\text{mol}^{-1}\cdot\text{K})$	249.2	51.71	291.5	16.17	41.7
$\Delta H (\text{kJ}\cdot\text{mol}^{-1}\cdot\text{K})$	106.1	55.25	116.9	43.02	51.62
$\tau_m (\mu\text{s})^a$	0.06	1.53	0.03	0.79	1.18

<sup>a</sup>At room temperature (298.15K).

experimental temperature range, which may be quite expected for the neutral Gd-complexes. On the other hand, two anionic Gd-complexes, Magnevisi<sup>®</sup> and Dotarem<sup>®</sup> reveal both slow- and fast-exchange regions depending on the temperature. Table 2 lists  $\Delta/\hbar$ ,  $\Delta S$ ,  $\Delta H$ , as well as  $\tau_m$  for **1** and **2**, and Figure 2 show a plot of  $\tau_m$  as a function of temperature. As might be expected from Figure 1, three neutral Gd-complexes show greater  $\tau_m$  values than their anionic counterparts. When the comparison is made among the first three, Omniscan<sup>®</sup> shows the greatest  $\tau_m$ , yet the differences are not great enough for  $\tau_m$  to play any significant role on the  $T_1$ -relaxivity.

### Conclusions

The EPR and  $^{17}\text{O}$  NMR measurements followed by theoretical calculation of the rotational correlation time ( $\tau_R$ ), the water residence time ( $\tau_m$ ), and the longitudinal electronic spin relaxation time ( $T_{1e}$ ) for **1** and **2** were carried out in order to investigate their efficiency as a paramagnetic contrast agent (PCA). Calculated parameters obtained in this study can be proved reasonable and acceptable as they are compared with the reported values for the related complexes. Of three parameters,  $\tau_R$  plays the most significant and contributing role on their very high  $T_1$ -relaxivities as compared to those for the clinically approved MRI CAs such as Magnevist<sup>®</sup>, Omniscan<sup>®</sup>, and Dotarem<sup>®</sup>. The unusually high  $\tau_R$  values for **1** and **2** can be explained in terms of the sterically demanding cyclohexyl group which may have caused retardation in the tumbling motion of the whole ligand.

**Acknowledgments.** This work was supported in part by the Ministry of Commerce, Industry and Energy (MOCIE) through the Mid Term Technology Development Program (grant No. 10028342) and through the Regional Technology Innovation Program (grant No. RTI04-01-01). Dr. A. Borel is gratefully acknowledged for the supply of the program used in this study. Dr. P. A. N. Reddy is also acknowledged for helpful discussion. Spectroscopic and analytical measurements were performed by KBSI.

### References

- Caravan, P. *Chem. Soc. Rev.* **2006**, *35*, 512.
- Vigouroux, C.; Belorizky, E.; Fries, P. H. *Eur. Phys. J. D.* **1999**, *5*, 243.
- Powell, D. H.; Dhubghaill, O. M. N.; Pubanz, D.; Helm, L.; Lebedev, Y. S.; Schlaepfer, W.; Merbach, A. E. *J. Am. Chem. Soc.* **1996**, *118*, 9333.
- González, G.; Powell, D. H.; Tissières, V.; Merbach, A. E. *J. Phys. Chem.* **1994**, *98*, 53.
- Vigouroux, C.; Bardet, M.; Belorizky, E.; Fries, P. H.; Guillenno, A. *Chem. Phys. Lett.* **1998**, *286*, 93.
- Caravan, P.; Ellison, J. J.; McMurry, T. J.; Lauffer, R. B. *Chem. Rev.* **1999**, *99*, 2293.
- Merbach, A. E.; Tóth, É. *The Chemistry of Contrast Agents in Medical Magnetic Resonance Imaging*, John Wiley & Sons, Ltd: Chichester, UK, 2001.
- Powell, D. H.; Merbach, A. E.; Gonzalez, G.; Brütcher, E.; Micskei, K.; Ottaviani, M. F.; Köhler, K.; von Zelewsky, A.; Grinberg, O. Y.; Lebedev, Y. S. *Helv. Chim. Acta.* **1993**, *76*, 2129.
- Powell, D. H.; Ni Dhubghaill, O. M.; Pubanz, D.; Helm, L.; Lebedev, Y. S.; Schlaepfer, W.; Merbach, A. E. *J. Am. Chem. Soc.* **1996**, *118*, 9333.
- Clarkson, R. B.; Smirnov, A. I.; Smirnova, T. I.; Kang, H.; Belford, R. L.; Earle, K.; Freed, J. H. *Mol. Phys.* **1998**, *96*, 1325.
- Borel, A.; Tóth, É.; Helm, L.; Janossy, A.; Merbach, A. E. *Phys. Chem. Chem. Phys.* **2000**, *2*, 1311.
- Borel, A.; Helm, L.; Merbach, A. E. *Chem. Eur. J.* **2001**, *7*, 600.
- Borel, A.; Yerly, F.; Helm, L.; Merbach, A. E. *J. Am. Chem. Soc.* **2002**, *124*, 2042.
- Rast, S.; Fries, P. H.; Belorizky, E. *J. Chem. Phys.* **2000**, *113*, 8724.
- Rast, S.; Borel, A.; Helm, L.; Belorizky, E.; Fries, P. H.; Merbach, A. E. *J. Am. Chem. Soc.* **2001**, *123*, 2637.
- Rast, S.; Fries, P. H.; Belorizky, E. *J. Chem. Phys.* **1999**, *96*, 1543.
- Dutta, S.; Park, J. A.; Jung, J. C.; Chang, Y. M.; Kim, T. J. *Dalton Trans.* **2008**, 2199.
- (a) Dutta, S.; Kim, S. K.; Patel, D. B.; Kim, T. J.; Chang, Y. M. *Polyhedron* **2007**, *26*, 3799. (b) Sk, M. N.; Park, J. A.; Chang, Y. M.; Kim, T. J. *Bull. Korean Chem. Soc.* **2008**, *29*, 1211.
- Dutta, S.; Kim, S. K.; Lee, E. J.; Kim, T. J.; Kang, D. S.; Chang, Y. M.; Kang, S. O.; Han, W. S. *Bull. Korean Chem. Soc.* **2006**, *27*, 1038.
- Belorizky, E.; Fries, P. H. *Phys. Chem. Chem. Phys.* **2004**, *6*, 2341.
- Micskei, K.; Helm, L.; Brütcher, E.; Merbach, A. E. *Inorg. Chem.* **1993**, *32*, 3844.
- Swift, T. J.; Connick, R. E. *J. Chem. Phys.* **1962**, *37*, 307.
- Tóth, É.; Connac, F.; Helm, L.; Adzamlı, K.; Merbach, A. E. *Eur. J. Inorg. Chem.* **1998**, 2017.